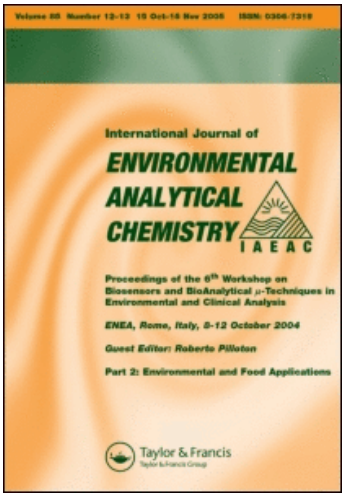

International Journal of Environmental Analytical Chemistry

Publication details, including instructions for authors and subscription information:
http://www.informaworld.com/smpp/title~content=t713640455

Self-quenching DNA probes based on dye dimerization for identification of mycobacteria

Jens-Peter Knemeyer[a]; Nicole Marmé[b]; Bernhard Häfner[c]; Gregor Habl[b]; Gabriela Schäfer[b]; Matthias Müller[c]; Oliver Nolte[c]; Markus Sauer[d]; Jürgen Wolfrum[b]

[a] Deutsches Krebsforschungszentrum, Abteilung funktionelle Genomanalyse, 69120 Heidelberg, Germany [b] Physikalisch-Chemisches Institut, Universität Heidelberg, 69120 Heidelberg, Germany [c] Hygiene-Institute, Dept. 17.1 Hygiene & Medical Microbiology, 69120 Heidelberg, Germany [d] Fakultät für Physik, Angewandte Laserphysik und Laserspektroskopie, Universität Bielefeld, 33615 Bielefeld, Germany

To cite this Article Knemeyer, Jens-Peter , Marmé, Nicole , Häfner, Bernhard , Habl, Gregor , Schäfer, Gabriela , Müller, Matthias , Nolte, Oliver , Sauer, Markus and Wolfrum, Jürgen(2005) 'Self-quenching DNA probes based on dye dimerization for identification of mycobacteria', International Journal of Environmental Analytical Chemistry, 85: 9, 625 — 637

To link to this Article: DOI: 10.1080/03067310500146094

URL: http://dx.doi.org/10.1080/03067310500146094

Intern. J. Environ. Anal. Chem.
Vol. 85, Nos. 9–11, 10 August–15 September 2005, 625–637

Taylor & Francis
Taylor & Francis Group

Self-quenching DNA probes based on dye dimerization for identification of mycobacteria

JENS-PETER KNEMEYER*†, NICOLE MARMÉ‡, BERNHARD HÄFNER§, GREGOR HABL‡, GABRIELA SCHÄFER‡, MATTHIAS MÜLLER§, OLIVER NOLTE§, MARKUS SAUER¶ and JÜRGEN WOLFRUM‡

†Deutsches Krebsforschungszentrum, Abteilung funktionelle Genomanalyse, Im Neuenheimer Feld 580, 69120 Heidelberg, Germany
‡Physikalisch-Chemisches Institut, Universität Heidelberg, Im Neuenheimer Feld 253, 69120 Heidelberg, Germany
§Hygiene-Institute, Dept. 17.1 Hygiene & Medical Microbiology, Im Neuenheimer Feld 324, 69120 Heidelberg, Germany
¶Fakultät für Physik, Angewandte Laserphysik und Laserspektroskopie, Universität Bielefeld, Universitätsstr. 25, 33615 Bielefeld, Germany

(*Received 29 December 2004; in final form 15 February 2005*)

This paper presents new self-quenching DNA probes that exploit the efficient fluorescence quenching by the formation of dye dimers. The probes consist of a hairpin-structured oligonucleotide that is labeled with two identical fluorescence dyes that are able to form non-fluorescent H-type dimers while the hairpin is closed. We used the oxazine derivative MR 121 that has a sufficient dimerization tendency and can be excited by a pulsed diode laser emitting at 635 nm. Upon hybridization to the target DNA, the dyes are separated and a 12-fold increase of the fluorescence intensity occurs. The probe was used for the specific detection of *Mycobacterium xenopi* in a model system. Specific target DNA and a control target, differing by six nucleotides were amplified by polymerase chain reaction (PCR). A confocal fluorescence microscope was used to observe the fluorescence bursts of individual probe molecules in the presence of target PCR product and controls. By experiment and by the respective simulation we demonstrated that the secondary structure of the target DNA hinders the hybridization to the DNA probe at room temperature. Based on these data a successful hybridization procedure was developed and allowing the detection of nanomolar concentrations of *Mycobacterium xenopi* specific target at room temperature, using single-molecule detection techniques.

Keywords: Self-quenching DNA probes; Single-molecule spectroscopy; Dye-dimerization

1. Introduction

Infectious diseases are the most frequent cause of death. Emerging infections and the tendency of microbes to develop antimicrobial resistance patterns, rapidly provide

*Corresponding author. Fax: +49-6221-424687. Email: J.Knemeyer@dkfz.de

International Journal of Environmental Analytical Chemistry
ISSN 0306-7319 print: ISSN 1029-0397 online © 2005 Taylor & Francis
DOI: 10.1080/03067310500146094

a growing challenge for routine diagnostic services. Rapid, reliable, economic and highly sensitive DNA detection methods have therefore become increasingly important in many fields, such as environmental studies, physical and biochemical research, or health care. They play a major role in early-stage diagnostics of cancer diseases, infections like HIV and tuberculosis, or antimicrobial resistance mechanisms.

Detection of specific DNA sequences can be classified into homogeneous and heterogeneous assay formats. In common heterogeneous assays fluorescently-labeled probes hybridize to the target-DNA that has been immobilized on a solid surface, e.g. by another hybridzation reaction [1, 2]. After removal of the unhybridized probes, through several cleaning steps, the remaining fluorescence intensity is measured. Unfortunately, the requirement of removing unhybridized probe molecules precludes the use of this technique for on-line monitoring of hybridization. In addition, unspecific adsorption of dye-labeled probes on the surface decreases the sensitivity of common heterogeneous assays. Homogeneous assays allow time-efficient detection of DNA without cleaning or separation steps. Basically, the probe consists of a short fluorescently-labeled oligonucleotide complementary to the target sequence. After hybridization to the target the diffusion time increases, due to the now higher mass and can be measured by FCS (Fluorescence Correlation Spectroscopy) [3, 4]. Other assays are based on double-labeled probes in which a FRET-pair (Fluorescence-Resonance-Energy-Transfer) is formed by the dyes [5]. More recent methods, like the molecular beacons developed by Tyagi and Kramer [6, 7], use probes that report the presence of a specific DNA sequence by a significant increase of their fluorescence intensity. These probes are based on oligonucleotides labeled with a fluorescent dye and a quencher molecule like DABCYL. The last 4–6 nucleic bases of each end of the oligonucleotide are complementary to one another. Thus the probe forms a hairpin-structure and the fluorescence dye and the quencher molecule are in close proximity, effecting an efficient quenching of the fluorescence intensity. The loop sequence of the hairpin-structured probe is complementary to the target-DNA. By hybridization to the target, a rigid double helix is formed and the hairpin is opened. Thus, the dye and quencher molecule lose contact and the fluorescence intensity increases. Optimization can be used for single nucleotide polymorphism (SNP) analysis [8]. Instead of organic quencher molecules like DABCYL or the more effective *black hole quencher* (BHQ) [9], gold nano-particle have been successfully applied [10]. Hence the fluorescence of several oxazine and rhodamine derivatives is quenched by the nucleic base guanosine [11–13], mono-labeled DNA-probes, called 'Smart Probes', have been developed [14]. Thereby, the dye-labeled end, e.g. the 5-prime, contains several cytosines and the opposite end contains accordingly several guanosine. In the closed hairpin form the guanosine quenches the fluorescence of the dye, whereas opening the hairpin leads to an increase of fluorescence intensity. The sensitivity of homogeneous assays can be enhanced to the pico-molar (10^{-12} M) range by applying single-molecule detection methods [15, 16]. By dint of these self-quenching probes it is possible to construct heterogeneous assays that do not require any cleaning or separation steps [17–19]. For example the smart probes were linked by a biotin–streptavidine system to a BSA coated glass surface and the fluorescence of the individual probes was detected by *fluorescence lifetime imaging microscopy* (FLIM) [20]. With this method a DNA-target concentration of 10^{-13} M can be detected [21].

Here we present novel hairpin-structured, doubly-labeled DNA-probes based on dye dimerization which consist of oligonucleotides labeled with identical dye molecules

at both ends. Thus the synthesis is less complicated than in the case of molecular beacons with two different labels. The advantage over the mono-labeled 'Smart Probes' is a more efficient quenching of the closed probe. Furthermore, we used these probes for the identification of *Mycobacterium xenopi*. In order to provide a model system the probes were used to specifically detect nanomolar amounts of *M. xenopi* specific DNA. *Mycobacterium xenopi* belongs to the large group of saprophytic mycobacteria. Reliable identification of the 101 different species in this group [22] by means of molecular methods is cumbersome, so new approaches are urgently needed.

2. Experimental

The oligonucleotides for the probe (5′-TACCGGGTTTTCTCGTGGTGACGGTA-3′) and the complementary target (5′-CCCCTACCGTCACCACGAGAAAACCCGCA G-3′) were purchased from IBA (Göttingen, Germany), in which the probe oligonucleotide is amino modified at the 5-prime (amino-C6-linker) as well as at the 3-prime (amino-C7-linker). The molecular structure and spectral properties of the fluorescence dye MR 121 that was kindly provided by K.H. Drexhage (Universität-Gesamthochschule Siegen, Germany), are shown in figure 1. Before coupling the dye to the amino-modified oligonucleotide and the lysine, the carboxyl group of the chromophore was converted into a N-hydroxysuccinimidyl ester by a 4 h reaction with an equimolar amount of N-(3-dimethylaminopropyl)-N-ethylcarbodiimide hydrochloride (EDC) and N-hydroxysuccinimide (NHS) in acetonitrile. For the coupling of the dyes to both amino groups of the oligonucleotide and the lysine respectively, 20 μL of a 0.1 mM aqueous solution of the amino acid was mixed in 50 μL of carbonate buffer (0.1 M, pH 8.5) with a 10-fold excess of the activated dye (20 μL; 1.0 mM in acetonitrile). The reaction solution was incubated for 12 h at room temperature, and the product was purified by HPLC (Hewlett-Packard, Böblingen, Germany) using a reversed-phase column (Knauer, Berlin, Germany) with octadecylsilanehypersil C18. Separation was performed in 0.1 M triethylammonium acetate, using a linear gradient from 0 to 75% acetonitrile in 20 min.

Absorption spectra were taken on a Cary 500 UV–VIS–NIR spectrometer (Varian, Darmstadt, Germany) using glass cuvettes with an optical pathway of 10 mm. Fluorescence spectra were performed using a Cary Eclipse fluorescence spectrometer (Varian, Darmstadt, Germany).

2.1 *DNA extraction and PCR*

Genomic DNA from *M. xenopi* and *M. fortuitum*, both isolated form respiratory tract specimens in our routine diagnostic facility, was extracted as described previously (Häfner *et al.*). Following extraction 10 μL of the respective DNA samples were used to amplify a fragment of the bacterial 16S rRNA gene with lengths of 260 bp (*M. xenopi*) and 248 bp (*M. fortuitum*). Primers used were '360F' (5′ CTC CGT CGT CAC CCC TTA TA 3′) and '600R' (5′ CAC CGT AAG GTG CTT GTT GC 3′), corresponding to *E. coli* 16S rRNA positions 348 to 367 and 615 to 596, respectively. The PCR was performed after an initial 5 min denaturation step at 94°C with 45 cycles of 94°C (45 s), 64°C (60 s) and 72°C (90 s) and a final extension at 72°C for 10 min. PCR reagents were obtained from MBI Fermentas (Vilnius, Lithuania).

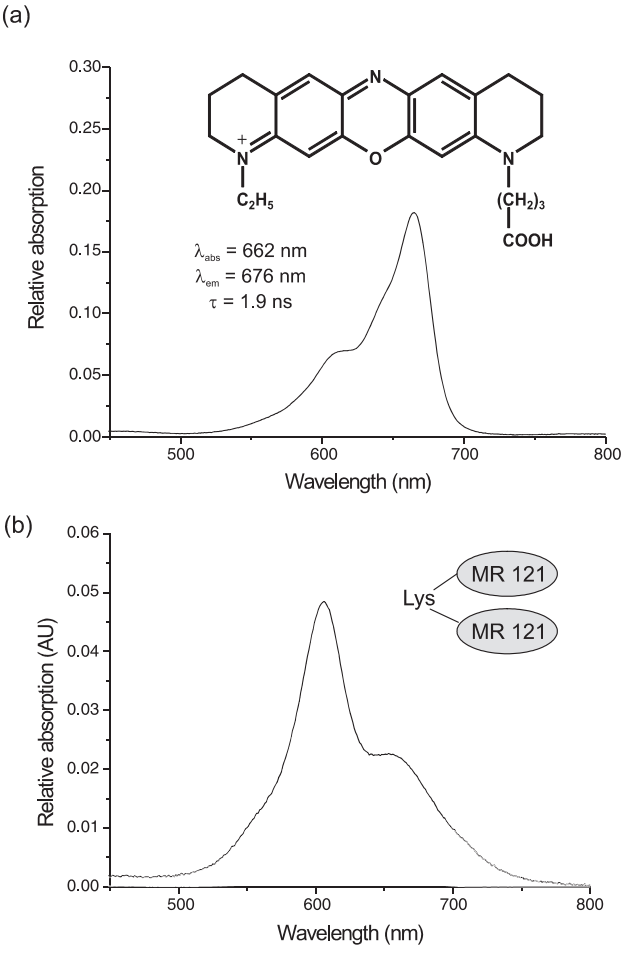

Figure 1. (a) Molecular structure and fluorescence properties of the oxazine derivative MR 121. (b) Absorption spectrum of a doubly-labeled lysine.

2.2 *Single-molecule experiments*

The experimental set-up for single-molecule experiments consists essentially of a standard inverse fluorescence microscope. A pulsed-diode laser emitting at 635 nm (PDL800B; Picoquant, Berlin, Germany) served as the excitation source. This laser system provides light pulses with a duration of less than 100 ps full width at half-maximum (FWHM) at a repetition rate of 80 MHz. The elliptical shape of the laser beam profile was converted into a circular (Gaussian-like) profile by the use of two cylindrical lenses. Passing an excitation filter (639DF9; Omega Optics, Brattleboro, VT) the collimated laser beam was directed into an inverted microscope (Axiovert 100TV; Zeiss, Germany) via the backport and coupled into an oil immersion objective ($100\times$ NA = 1.4; Nikon, Japan) by a dichroic beam splitter (645DMLP; Omega Optics, Brattleboro, VT). The average laser power was adjusted with neutral density filters to be 700 μW at the sample. Fluorescence light was collected with the same objective and focused through the TV outlet of the microscope onto a 100-μm pinhole.

Fluorescence light passing the pinhole was imaged onto the active area of an avalanche photodiode (AQR-14; EG&G, Canada). The detector signal was registered by a PC plug-in card for time-correlated single-photon counting (TCSPC) (SPC-630; Becker&Hickl, Berlin, Germany). From the data of the TCSPC card, *multichannel-scalar* (MCS) traces were generated. For this, all photons detected within a millisecond were added up to a bin of the MCS trace. The raw data are shown in figure 6 without modification by any filtering algorithm. Each peak (fluorescence burst) is due to a fluorescent probe passing the detection volume. For analyses of the MCS traces, a peak recognition filter extracting bursts that have a maximum intensity of more than 16 kHz was applied. For each burst found the burst duration (in milliseconds), maximum intensity, overall intensity (total number of photons) and the fluorescence lifetime are stored.

3. Results and discussion

The novel DNA probes are based on the formation of dye-dimers from which we have had to evaluate suitable fluorescent dyes first. We found the oxazine derivative MR 121 to be a good candidate. It has an absorption maximum of 662 nm and can be excited with a pulsed red laser diode (635 nm). Its structure and absorption spectrum is shown in figure 1(a). Furthermore, MR 121 has a sufficient tendency to form non-fluorescent H-type dimers. To investigate the properties of the dimer two MR 121 dyes were labeled to the amino groups of a lysine. Due to the close proximity most of the chromophores are part of a dimer. The resulting absorption spectrum is shown in figure 1(b). The absorption maximum now lies at 608 nm and is therefore shifted to shorter wavelength compared to the monomeric dye, as predicted in the excitation theory [23, 24] for non-fluorescent H-type dimers. The remaining fluorescence of the sample is less than 2% compared to the fluorescence intensity of the same amount of free dye.

For preparing the DNA probes two dyes were attached to a hairpin-structured oligonucleotide with a stem that contains five base pairs. The sequence of the stem is designed in such a way that less guanosine residues are possible in close proximity to the dyes, because the fluorescence intensity of the oxazine derivative MR 121 is efficiently quenched by guanosine. Furthermore, wide parts of the stem should be complementary to the target sequence, so that they contribute to the stability of the probe–target complex. Figure 2 shows the working mechanism as well as the spectroscopic properties of the probe. The fluorescence intensity of the probe is efficiently quenched in the closed form due to the formation of non-fluorescent dye dimers. The absorption band at 608 nm is higher than the band at the absorption maximum of the free dye (650 nm) indicating a high percentage of dye dimers. The green sequence is complementary to the target sequence. Upon hybridization a rigid double helix is formed, thus the proximity of the dyes is lost affecting a ten-fold increase of the fluorescence intensity. The absorption spectrum shows no evidence of remaining in the dye dimers.

In order to evaluate suitable reaction conditions for the hybridization of the probe to the target sequence the salt concentration of the reaction buffer was varied. A high salt concentration is advantageous for this assay system. The hybridization to the target sequence is accelerated significantly by increasing the concentration of NaCl.

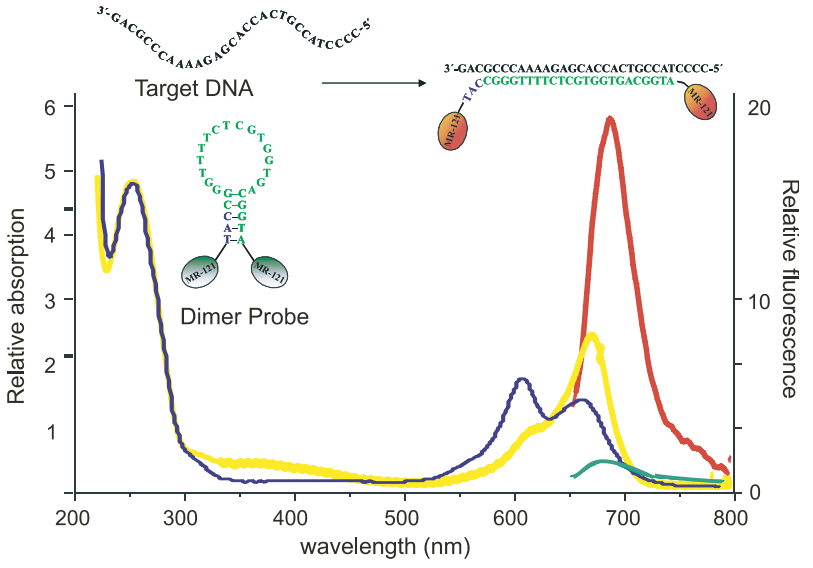

Figure 2. Working mechanism and spectroscopic properties of the dimer-probes. Blue: absorption spectrum of the dimer probe in 2 M NaCl; green: fluorescence spectrum of the dimer probe; yellow: absorption spectrum of dimer probe opened by adding acetonitrile; red: fluorescence spectrum after hybridization to the target DNA.

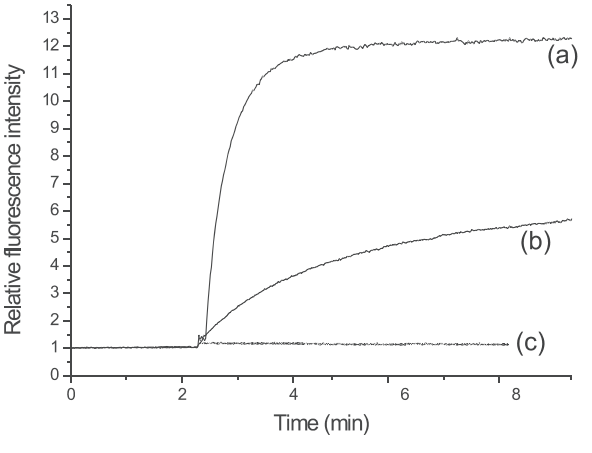

Figure 3. Fluorescence increase of the 10^{-7} M dimer probe in a Tris-HCl buffer (pH 7.0) containing (a) 2 M and (b) 300 mM NaCl after adding a three-fold excess of the target sequence of the *M. xenopi*. As a control, the respective sequence of the *M. fortuitum* that differs by six base pairs was added (c). The excitation wavelength is 650 nm, and the emission wavelength 680 nm, respectively.

Figure 3 shows the fluorescence increase after adding a three-fold excess of target DNA to a 10^{-7} M dimer probe in a Tris-HCl buffer (pH 7.0) containing 2 M NaCl, and 300 mM NaCl respectively. The effect of $MgCl_2$ is smaller and can be neglected, especially at high NaCl concentrations (data not shown). Increasing the NaCl concentration also raises the percentage of dimers leading to more efficient fluorescence quenching of the probe and thus to a higher fluorescence increase after hybridization to the target

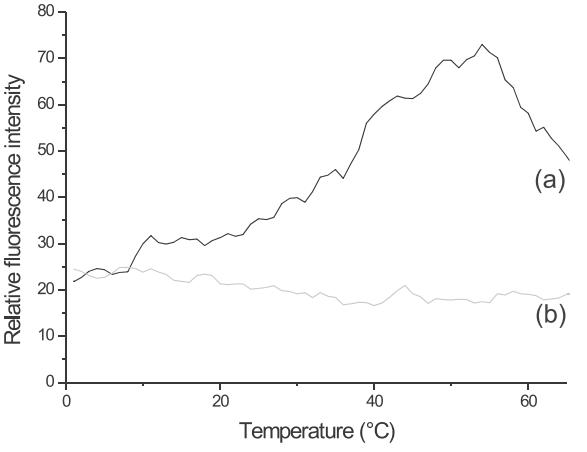

Figure 4. Fluorescence signal of 10^{-8} M dimer probe in a Tris-HCl buffer pH 7.0 containing 2 M NaCl in the presences of an equimolar amount of PCR product of (a) *M. xenopi* and (b) *M. fortuitum*. The temperature is increased by $1^{\circ}C\,min^{-1}$ whereas the excitation wavelength (650 nm) and the emission wavelength (680 nm) stay constant.

DNA. However, at salt concentrations below 30 mM NaCl no significant dimerization can be observed although the hairpin is closed. Under these conditions the melting point of the probe was calculated to 47.6°C. In the presence of 300 mM NaCl a six-fold increase of the fluorescence intensity occurs in 10 min, whereas 2 M NaCl produces a 12-fold increase within 2 min. The necessity of salts for the formation of MR 121 dimers might be due to the positive charge of the dye. The dyes should electrostatically repulse each other and are attracted to the negatively-charged DNA backbone. Thus an efficient dimerization could be hindered. Anyway, increasing salt concentration reduces electrostatical interactions and favors the dimerization of MR 121 dyes covalently linked to DNA.

In contrast to the short custom synthesized target DNA, the addition of PCR product does not result in an increase of fluorescence intensity at room temperature. Therefore, a sample containing 10^{-8} M dimer probe in Tris-HCl buffer (pH 7.0) and 2 M NaCl were mixed with an equimolar amount PCR product of *M. xenopi*. As a control, amplified target DNA from *M. fortuitum*, containing six mismatches (program FindPatterns, HUSAR program package, DKFZ Heidelberg, Germany) with respect to the *M. xenopi* PCR product, was used. The PCR product was denaturated at 95°C for 5 min and chilled on ice prior to use in the assay. The fluorescence signals of both samples were measured at increasing temperature. Thereby, the excitation wavelength (650 nm) as well as the emission wavelength (680 nm) stayed constant. The temperature is increased by $1^{\circ}C\,min^{-1}$. Figure 4 shows that almost no fluorescence increase and thus no efficient hybridization reaction occur below 20°C. With increasing temperature the hybridization process accelerates and reaches a maximum at approximately 50°C. At even higher temperatures the fluorescence signal decreases because the melting point of the probe target hybrid is transgressed whereas the melting point of the hairpin probe (65°C) is not yet reached. Thus the probe is removed from the target DNA and a hairpin structure in which the fluorescence is quenched is formed again. Under the same conditions the dimer probe hybridizes completely to the short custom synthesized target DNA even at 0°C and the fluorescence signal show no significant dependence on the

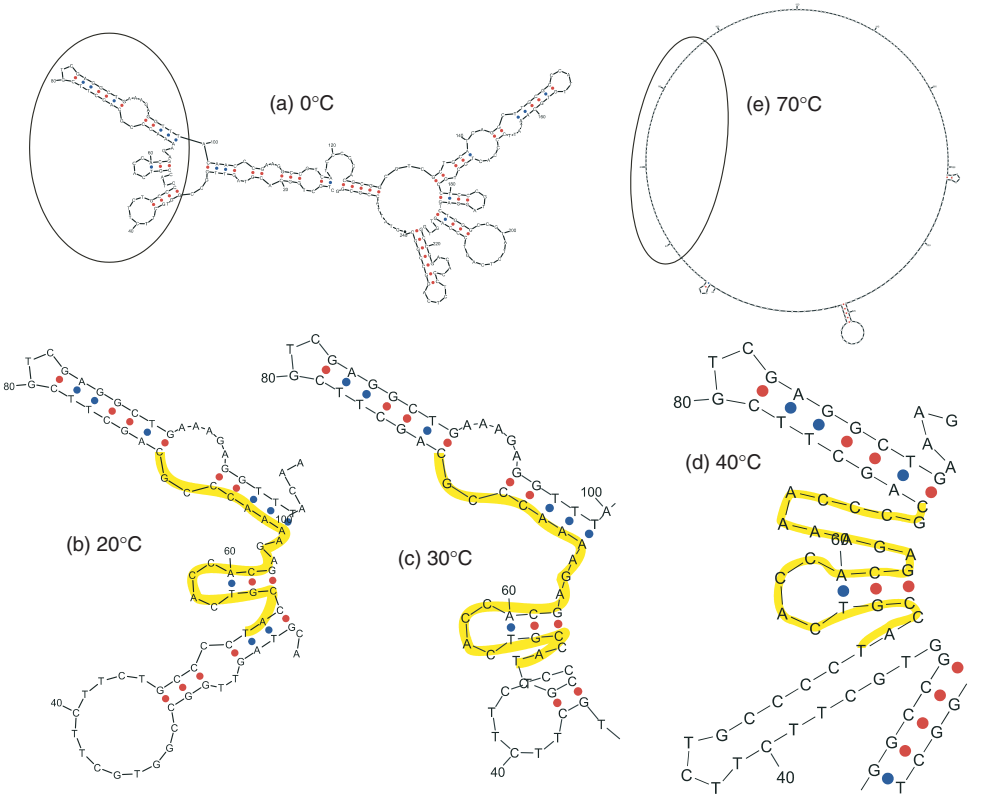

Figure 5. Secondary structures of the target DNA-strand pf the PCR-product of *M. xenopi* calculated by the *m*-fold program of Zucker and Turner. They are simulated for 1 M NaCl at (a) 0°C, (b) 20°C, (c) 30°C, (d) 40°C and (e) 70°C. The blue points represents AT base pairs, red point GC base pairs. The target sequence of the DNA probe is marked yellow.

temperature except for the decrease over 50°C (data not shown). To comprehend this behavior we calculated the secondary structure of the single-stranded PCR product. Therefore, the *m*-fold program of Zucker and Turner was used [25, 26]. Figure 5 shows the structures of the PCR fragment of *M. xenopi* consisting of 260 nucleic bases for different temperatures and a 1 M NaCl concentration. For 0 and 70°C the structure of the hole PCR fragment is illustrated, whereas for 20, 30 and 40°C only a cut-out containing the target sequence (yellow marked) of the DNA probe is shown. At 0°C more than 50% of the single-stranded PCR product is existent as a double helix. Also the target sequence is not single stranded. Fifteen of the 24 nucleic bases are involved in three different double-helical structures and even increasing the temperature to 20°C does not change the structure of the target region. Thus the hybridization of the dimer probe is strongly hindered which is consistent with the experiment in which no significant hybridization was observed up to 20°C (figure 4). At 30°C one of the double helix motives containing three nucleic bases of the target sequence is melted, but 50% of the bases are still involved in two double helices. The second helix is melted at 40°C thus 18 nucleic bases are single stranded and only three base pairs remain in the target region. This last hairpin motive should be

opened by the hybridization of the dimer probe that contains 24 matching nucleic bases. That is concordant with the experimental data that show efficient hybridization of the probe above 40°C. The lowest concentration of PCR product that can be detected by measurements with standard fluorescence spectrometers is about 10^{-8} M. In order to raise the sensitivity we used single-molecule spectroscopy. While ensemble measurements yield only information on the average properties, single-molecule experiments allow the characterization of individual molecules [27–29]. Thus, often different subpopulations in heterogeneous mixtures can be identified. This feature might also be useful for the discrimination of closed, quenched dimer probes and open, fluorescent dimer probes that are hybridized to the target DNA. For single-molecule experiments the dimer probe was diluted in 2 M NaCl to a concentration of approximately 10^{-9} M. Hence, on average less than one molecule is the 1 μm^3 detection volume where the measured fluorescence signal is usually caused by a single molecule. Figure 6 shows the signal binned in 1 ms intervals for the dimer probe in the absence and in the presence of the respective PCR products. As a matter of clarity a 2 s cutout of each measurement is illustrated in which single fluorescence bursts can be seen. In the absence of any DNA target sequences only a few fluorescence bursts reach a count rate of more than 40 kHz. The relatively low number of detected fluorescence bursts indicates an efficient quenching of the dimer probes. Ninety microlitres of the 10^{-9} M dimer probe solution was mixed with 10 µL of the 5×10^{-9} M PCR product of *M. xenopi* and *M. fortuitum*, respectively, so that the concentration of the PCR product was approximately 5×10^{-10} M. After 15 min of incubation at 50°C the mixture is transferred to a 170 µm thick glass cover slide located above the microscope objective. There is no significant difference between the MCS traces of the pure dimer probe and the sample containing the PCR product of the *M. fortuitum* that does not match the dimer probe. The sample of the *M. fortuitum* shows slightly less fluorescence signals due to dilution effects and perhaps different adsorptions at surfaces or plastic pipettes used for adding and mixing the PCR product. In this sample some signals with intensities above 70 kHz can be observed that might be due to unspecific hybridization. Whereas signals of the pure dimer probe never reach these count rates. Significantly more and also more intensive fluorescence bursts are observed for the sample of the PCR product of *M. xenopi* containing the matching target sequence (figure 6c). The overall intensity that can be calculated by summing all detected photons increases by a factor of two meaning that less than 20% of the dimer probes are opened. The burst analysis program found in the 100 s long MCS traces for the pure dimer probe that 995 bursts achieved a maximum intensity of 16 kHz, for *M. fortuitum* 852 bursts and for *M. xenopi* 2413 bursts. As can be seen in figure 6(c) hybridization to the target DNA affects not only more fluorescence bursts per time, but also more intensive and broader bursts. Before and after hybridization to the target DNA the fluorescence lifetime is about 2.6 ns (data not shown), which is significantly longer than the lifetime of the free dye (1.9 ns). The longer lifetime is due to interaction between the dye and the nucleic bases. MR 121 coupled to an oligonucleotide consisting only of adenine, cytosine and tymidine shows a lifetime of approximately 3.0 ns, but it is shortened by the nucleic base guanosine. To demonstrate the change of the burst intensities, histograms of the total number of photons of each burst were created (figure 7). A useful discrimination can be achieved by counting the fluorescence bursts above a certain intensity threshold level. We found a burst size of 100 photons to be a good threshold because no burst of the closed dimer probe reaches that value.

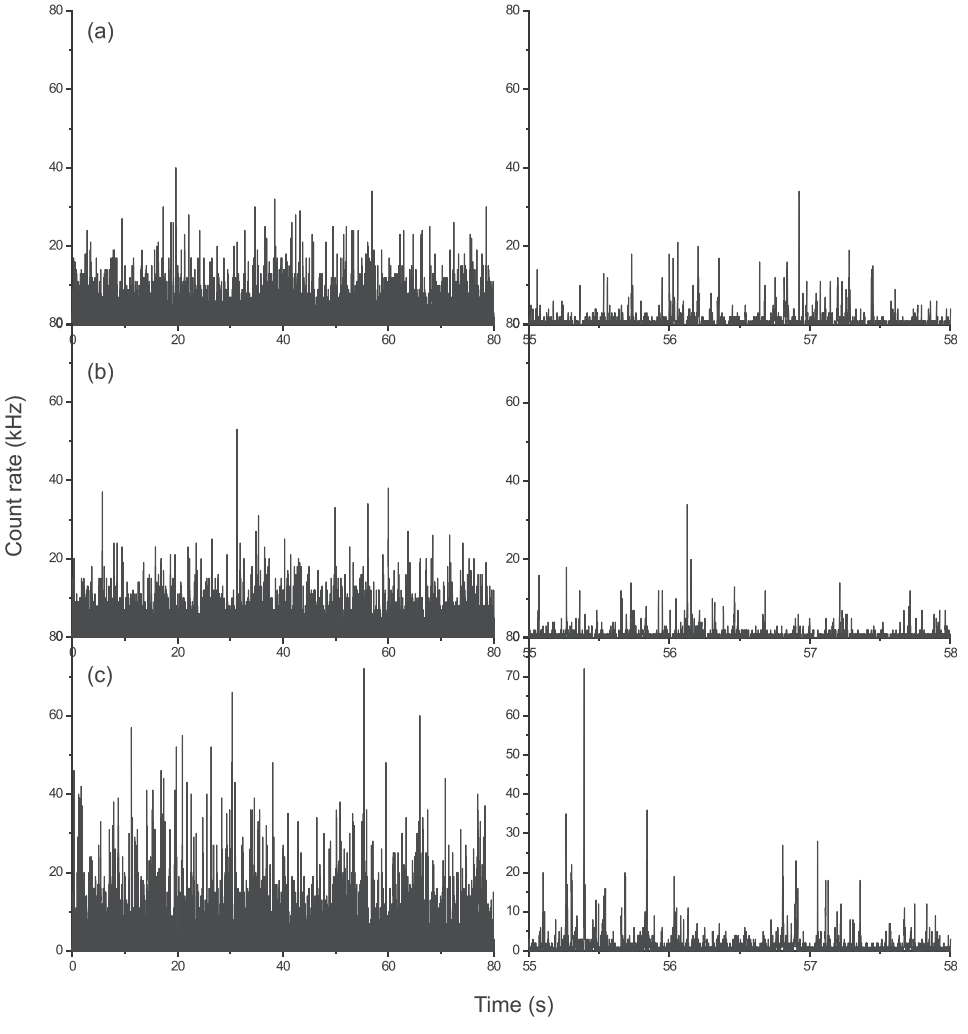

Figure 6. Fluorescence intensity traces of the 1×10^{-9} M dimer probe in 2 M NaCl in the absence (a) and in the presence of 5×10^{-10} M PCR product of (b) *M. fortuitum* and (c) *M. xenopi* and the respective cut-outs. The binwidth is 1 ms.

The *M. fortuitum* sample generates just five bursts within 100 s, whereas for the *M. xenopi* sample more than 200 bursts were detected.

4. Conclusion

We have synthesized new self-quenching DNA probes that exploit the efficient fluorescence quenching by formation of dye dimers and applied them for the identification of specific mycobacteria in a homogeneous assay. The probes consist of a hairpin-structured oligonucleotide that is labeled with two identical fluorescence dyes. In contrast to molecular beacons that require a specific labeling, with both a dye and a quencher molecule the synthesis of the dimer probes is drastically simplified.

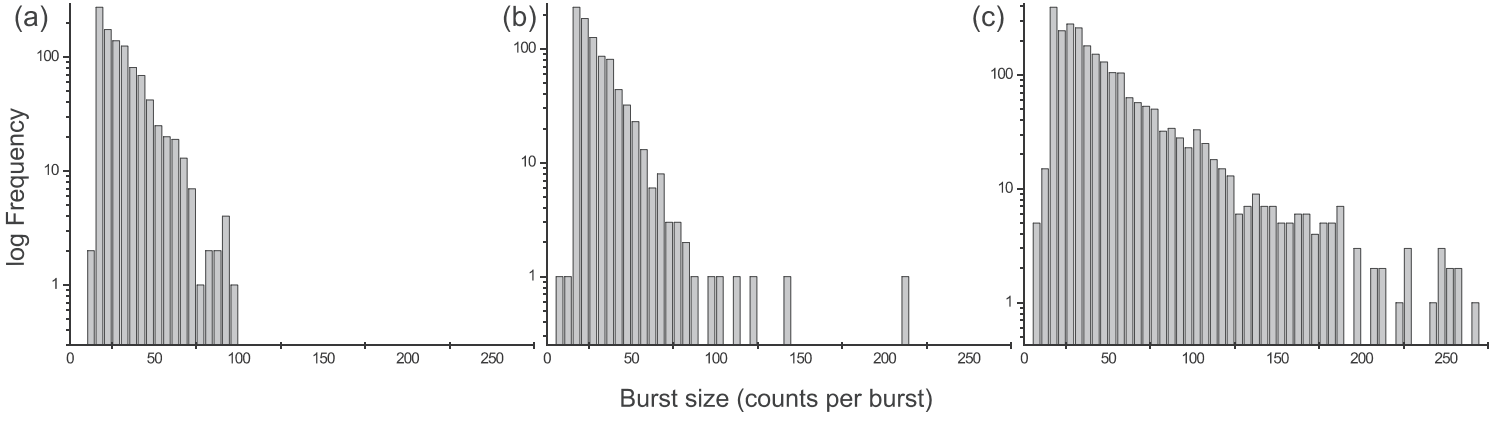

Figure 7. Histograms of the burst size (number of photons per burst) for (a) the pure dimer probe, (b) the sample containing the PCR-product of *M. fortuitum* and (c) the sample containing the PCR product of *M. xenopi*. The bursts of the MCS traces shown in figure 6 that reach a maximum intensity of 16 kHz were considered.

Indeed the synthesis of the Smart Probes is even simpler because they need only one dye and use the oligonucleotide itself as a quencher, but the dimer probes exhibit a more efficient quenching mechanism and thus the increase of the fluorescence intensity after hybridization to the target DNA is significantly higher. Furthermore, traces of free dye remaining from the synthesis or generated by decomposed probes do not interfere in the assay. In the case of molecular beacons or Smart Probes each free dye may simulate a hybridized probe, whereas the signal of a hybridized dimer probe is twice as high as the signal produced by free dyes.

Moreover, we demonstrated that the secondary structure of the target DNA is often able to hinder the hybridization of the probe to the target. In this article we optimized the reaction condition by simulating the temperature dependence of the secondary structure of the target DNA.

Acknowledgements

We thank K.-H. Drexhage for the generous disposal of the oxazine derivative MR 121 and Heike Böhm for carefully reading the manuscript. For financial support we thank the Landesstiftung Baden-Württemberg. M.S. and O.N. are supported by grant 13N8439 and 13N8438 of the Bundesminister für Bildung und Forschung (BMBF), respectively.

References

[1] F.M. Ausubel, R. Brent, R.E. Kingston, D.D. Moore, J.G. Seidman, J.A. Smith, K. Struhl. *Current Protocols in Molecular Biology*, John Wiley & Sons, New York (1994).
[2] F.F. Chehab, Y.W. Kann. *Proc. Natl. Acad. Sci. USA*, **86**, 9178 (1989).
[3] N.J. Gibson, H.L. Gillard, D. Whitcombe, R.M. Ferrie, C.R. Newton, S. Little. *Clin. Chem.*, **43**, 1336 (1997).
[4] M. Kinjo, R. Rigler. *Nucleic Acid Res.*, **23**, 1795 (1995).
[5] L.E. Morrison, T.C. Halder, L.M. Stols. *Anal. Biochem.*, **183**, 231 (1989).
[6] S. Tyagi, F.R. Kramer. *Nat. Biotechnol.*, **14**, 303 (1996).
[7] G. Bonnet, S. Tyagi, A. Libchaber, F.R. Kramer. *Proc. Natl. Acad. Sci. USA*, **96**, 6171 (1999).
[8] S.A.E. Marras, F.R. Kramer, S. Tyagi. *Genet. Anal.*, **14**, 151 (1999).
[9] G. Yao, W. Tan. *Anal. Biochem.*, **331**, 216 (2004).
[10] B. Dubertret, M. Calame, A. Libchaber. *Nat. Biotechnol.*, **19**, 365 (2001).
[11] M. Sauer, K.T. Han, R. Müller, S. Nord, A. Schulz, S. Seeger, J. Wolfrum, J. Arden-Jacob, G. Deltau, N.J. Marx, K.H. Drexhage. *J. Fluoresc.*, **5**, 247 (1995).
[12] U. Lieberwirth, J. Arden-Jacob, K.H. Drexhage, D.P. Herten, R. Müller, M. Neumann, A. Schulz, S. Siebert, G. Sagner, S. Klingel, M. Sauer, J. Wolfrum. *Anal. Chem.*, **70**, 4771 (1998).
[13] M. Sauer, K.H. Drexhage, U. Lieberwirth, R. Müller, S. Nord, C. Zander. *Chem. Phys. Lett.*, **284**, 153 (1998).
[14] T. Heinlein, J.P. Knemeyer, O. Piestert, M. Sauer. *J. Phys. Chem. B*, **107**, 7957 (2003).
[15] J.P. Knemeyer, N. Marmé, M. Sauer. *Anal. Chem.*, **72**, 3717 (2000).
[16] A. Castro, J.G.K. Williams. *Anal. Chem.*, **69**, 3915 (1997).
[17] X. Liu, W. Tan. *Anal. Chem.*, **71**, 5054 (1999).
[18] F.J. Steemers, J.A. Ferguson, D.R. Walt. *Nat. Biotechnol.*, **18**, 91 (2000).
[19] M. Culha, D.L. Stokes, G.D. Griffin, T. Vo-Dinh. *Biosens. Bioelectron.*, **19**, 1007 (2004).
[20] P. Tinnefeld, V. Buschmann, D.P. Herten, K.-T. Han, M. Sauer. *Single Mol.*, **3**, 215 (2000).
[21] O. Piestert, H. Barsch, V. Buschmann, T. Heinlein, J.P. Knemeyer, K.D. Weston, M. Sauer. *Nano Lett.*, **3**, 979 (2003).
[22] J.P. Euzéby. *Int. J. Syst. Bacteriol.*, **47**, 590 (1997).
[23] M. Kasha. *Radiat. Res.*, **20**, 55 (1963).
[24] V.I. Yuzhakov. *Russian Chem. Rev.*, **48**, 1076 (1979).
[25] M. Zuker. *Nucleic Acids Res.*, **31**, 3406 (2003).

[26] N. Peyret, Prediction of nucleic acid hybridization: Parameters and algorithms. PhD dissertation, Wayne State University, Department of Chemistry, Detroit, MI (2000).
[27] W.P. Ambrose, P.M. Goodwin, J.H. Jett, A. Van Orden, J.H. Werner, R.A. Keller. *Chem. Rev.*, **99**, 2929 (1999).
[28] J. Schaffer, A. Volkmer, C. Eggeling, V. Subramanian, G. Striker, C.A.M. Seidel. *J. Phys. Chem. A*, **103**, 331 (1999).
[29] A.A. Deniz, M. Dahan, J.R. Grunwell, T. Ha, A.E. Faulhaber, D.S. Chemla, S. Weiss, P.G. Schultz. *Proc. Natl. Acad. Sci. USA*, **96**, 3670 (1999).